Article

Discovery Medicine 2025; 37(200): 1961–1973
https://doi.org/10.24976/Discov.Med.202537200.169

Dissecting the Role of CKAP2L in Ovarian Cancer: Insights Into Cellular Dynamics and Immune Microenvironment Regulation

Ziyao Ren[1,2,3], Junnan Li[3], Zhouliang Yang[4], Hongkai Shang[2,*]

[1]School of Medicine, Zhejiang University, 310030 Hangzhou, Zhejiang, China
[2]Department of Gynecology, Hangzhou First People's Hospital Affiliated to Zhejiang University, 310006 Hangzhou, Zhejiang, China
[3]Department of Gynecology, The First People's Hospital of Yongkang, 321300 Yongkang, Zhejiang, China
[4]Department of Pathology, The First People's Hospital of Yongkang, 321300 Yongkang, Zhejiang, China
*Correspondence: shanghongkai_285nh@163.com (Hongkai Shang)
Submitted: 30 June 2025 Revised: 21 August 2025 Accepted: 2 September 2025 Published: 20 September 2025

Background: Cytoskeleton-associated protein 2-like (CKAP2L) has been implicated in various malignancies, including ovarian cancer. However, its role in modulating the immune microenvironment of ovarian cancer remains poorly understood. This study aimed to investigate the role of CKAP2L in regulating ovarian cancer cell proliferation, migration, and apoptosis.

Methods: The impact of CKAP2L knockdown on ovarian cancer cells and the immune microenvironment was examined. CKAP2L was silenced in ovarian cancer cell lines, and subsequent effects on proliferation, migration, and apoptosis were assessed. Macrophage polarization differentiated from peripheral blood mononuclear cells (PBMCs) co-cultured with ovarian cancer cells was evaluated. Expression of the adenosine A2A receptor (ADORA2A) in macrophages, and interleukin-1β (IL-1β), interleukin-10 (IL-10) and vascular endothelial growth factor (VEGF) levels in ovarian cancer cells, were analyzed using western blotting and cytokine antibody arrays.

Results: CKAP2L knockdown significantly reduced proliferation and migration of ovarian cancer cell, while promoting apoptosis ($p < 0.01$). Flow cytometry revealed that CKAP2L knockdown inhibited M2-type and promoted M1-type polarization of PBMC-derived macrophages induced by ovarian cancer cells ($p < 0.001$). Furthermore, CKAP2L knockdown reduced ADORA2A expression in macrophages, increased IL-1β secretion, and reduced IL-10, VEGF secretion by ovarian cancer cells ($p < 0.01$).

Conclusions: CKAP2L promotes ovarian cancer progression by enhancing proliferation and migration while suppressing apoptosis. It also regulates the immune microenvironment by influencing macrophage polarization and cytokine secretion. These findings highlight the pivotal role of CKAP2L in the pathogenesis of ovarian cancer and support its potential as a therapeutic target for regulating tumor growth and immune responses.

Keywords: ovarian cancer; cytoskeleton-associated protein 2 like; immune microenvironment; adenosine A2A receptor

Introduction

Ovarian cancer, one of the most lethal gynecological malignancies worldwide, arises from the epithelial cells of the ovary [1]. In China, the annual incidence of ovarian cancer is approximately 4.77 cases per 100,000 women, with a mortality rate of about 2.88 cases per 100,000, reflecting both high morbidity and mortality [2]. Hormonal imbalances, genetic predisposition, and environmental factors have been implicated in ovarian cancer development [3]. Clinically, the disease often presents with non-specific symptoms and is typically diagnosed at an advanced stage, leading to poor prognosis and frequent intraperitoneal metastasis [4]. Current treatment strategies primarily rely on surgical resection, chemotherapy, and targeted therapy. Traditional platinum- and taxane-based chemotherapy shows limited efficacy, with nearly 70% of patients relapsing within two years [5]. Poly (ADP-ribose) polymerase (PARP) inhibitors, such as olaparib, have been approved as maintenance therapy for advanced ovarian cancer following response to first-line chemotherapy [6]. Although surgery and chemotherapy significantly improve patient survival, prognosis remains poor due to recurrence and drug resistance. Recently, immune checkpoint blockade therapies have demonstrated significant clinical benefits across multiple malignancies [7]. Increasing evidence indicates that the immune microenvironment plays a crucial role in the onset and progression of ovarian cancer [8]. Thus, understanding its interactions with ovarian cancer is essential for identifying novel therapeutic targets for ovarian cancer.

Cytoskeleton-associated protein 2-like (CKAP2L) is a cytoskeleton-regulating protein primarily involved in microtubule organization [9]. It plays essential roles in bi-

Copyright: © 2025 The Author(s). Published by Discovery Medicine. This is an open access article under the CC BY 4.0 license.
Note: *Discovery Medicine* stays neutral with regard to jurisdictional claims in published maps and institutional affiliations.

ological processes, including cell cycle regulation, migration, and division [10]. CKAP2L influences cell morphology and function by regulating microtubule stability and dynamics [11]. In lung cancer, CKAP2L interacts directly with RNA polymerase II to regulate transcriptional elongation of key genes controlling the spindle assembly checkpoint, chromosome segregation, cell cycle progression, and E2F signaling, thereby promoting non-small cell lung cancer [9]. In breast cancer, CKAP2L is transcriptionally regulated by forkhead box P3 (FOXP3), which activates the protein kinase B/mechanistic target of rapamycin (AKT/mTOR) signaling pathway, promoting tumor development [12]. Notably, mTOR inhibition may extend healthy lifespan by mitigating inflammation associated with viral infection and autoimmune disease [13]. In glioma, CKAP2L has been identified as an independent risk factor, suppressing proliferation and invasion through downregulation of cell cycle-related proteins [14]. In ovarian cancer, insulin-like growth factor 2 mRNA-binding protein 2 (IGF2BP2) upregulates CKAP2L expression in an m6A-dependent manner, enhancing proliferation, migration, and invasion of ovarian cancer cells *in vitro*, while accelerating tumor growth and metastasis *in vivo* [15]. However, limited research exists about the role of CKAP2L in regulating the immune microenvironment of ovarian cancer.

Our analysis using the Tumor Immune Estimation Resource (TIMER) database revealed that CKAP2L expression positively correlates with macrophage infiltration and antigen presentation. Recent findings show that KIF20A deficiency significantly inhibits the progression of ovarian cancer through regulation of the phosphatase and tensin homolog (PTEN) signaling pathway and suppression of M2 macrophage polarization [16], underscoring the key role of macrophage polarization in the ovarian cancer microenvironment. Based on these observations, we hypothesized that CKAP2L promotes ovarian cancer progression by driving tumor cell proliferation and inducing immunosuppression through ADORA2A-dependent M2 macrophage polarization. In this study, we evaluated the role of CKAP2L in regulating the proliferation, migration, and apoptosis of ovarian cancer cell lines (OVCAR3 and Caov-3). Additionally, we investigated to study the effects and mechanisms of CKAP2L on the immune phenotype transformation from M1 to M2 of PBMC-derived macrophages induced by ovarian cancer cells.

Materials and Methods

Cell Culture

The human ovarian cancer cell lines OVCAR3 (HTB-161) and Caov-3 (HTB-75) were obtained from the American Type Culture Collection (ATCC, Manassas, VA, USA). The OVCAR3 cell line, derived from malignant ascites of patients with progressive ovarian adenocarcinoma, is widely used as a model of high-grade serous carcinoma (HGSC), the most aggressive and prevalent histological subtype [17]. Caov-3 cells, derived from ovarian adenocarcinoma tissue, were selected for their clinical relevance to major ovarian cancer subtypes [18]. Human peripheral blood mononuclear cells (PBMCs) were purchased from AnWei-sci (HUM-AWP-i010, Shanghai, China). Mycoplasma testing and short tandem repeat (STR) profiling were performed on cell lines, whereas PBMCs were not analyzed for STR. The detection result for Mycoplasma was negative. OVCAR3, Caov-3, and PBMCs were cultured in Roswell Park Memorial Institute Medium 1640 (RPMI-1640; 11875093, Thermo Fisher Scientific, Waltham, MA, USA) supplemented with penicillin G (100 µg/mL; 61-33-6, MCE, Monmouth Junction, NJ, USA), streptomycin (50 µg/mL; C0222, Biotop, Shanghai, China), and 10% fetal bovine serum (FBS; 5670701, Thermo Fisher Scientific, Waltham, MA, USA). All cultures were maintained at 37 °C in a humidified incubator with 5% CO_2.

Cell Transfection

Small interfering RNAs (siRNAs) targeting CKAP2L (siCKAP2L-1, GGAUCGAAGGAAACAACUATT, siCKAP2L-2, GGUUAAUAGGAGUCAAUAUTT) and a negative control siRNA (siNC, ACGUCACACGUUCGGAGAATT) were obtained from VIEWSOUD Biotech (Beijing, China). Ovarian cancer cells were divided into three groups: Con, siNC, and siCKAP2L. Cells (5×10^5) were transfected with 25 nM siCKAP2L or siNC using Lipofectamine 2000 (11668019, Thermo Fisher Scientific, Waltham, MA, USA) following the manufacturer's instructions. After 48 hours of incubation, transfected cells were harvested for subsequent experiments. Transfection efficiency was determined by RNA extraction and quantitative real-time polymerase chain reaction (qRT-PCR).

Cell Co-Culture

PBMCs were assigned to four groups: PBMC, Con cancer cell + PBMC, siNC cancer cell + PBMC, and siCKAP2L cancer cell + PBMC. As described previously [19], PBMCs were differentiated into macrophages. Briefly, PBMCs (1×10^6) were cultured in 2 mL of RPMI-1640 medium supplemented with 100 nM phorbol 12-myristate 13-acetate (PMA, HY-18739, MCE, CA, USA) for three days. After incubation, adherent cells were washed three times with phosphate-buffered saline (PBS; C0221A, Biotop, Shanghai, China) to remove non-adherent cells. To prevent direct cell-to-cell contact, PBMC-derived macrophages were co-cultured with OVCAR3 or Caov-3 cells (1×10^5 upper chamber) using Transwell inserts (FTW001, Biotop, Shanghai, China; pore size 0.4 µm) [20]. In the Con cancer cell + PBMC group, non-transfected OVCAR3 or Caov-3 cells were co-cultured with PBMCs. In the siNC cancer cell + PBMC group, OVCAR3 or Caov-3 cells transfected with siNC were co-cultured with PBMCs. In the siCKAP2L cancer cell + PBMC group, OVCAR3 or

Caov-3 cells transfected with siCKAP2L were co-cultured with PBMCs. All chambers were then incubated at 37 °C for 36 hours.

The Cancer Genome Atlas (TCGA)

The diagnostic potential of CKAP2L in ovarian cancer was evaluated using receiver operating characteristic (ROC) curve analysis with data obtained from the TCGA database (https://tcga-data.nci.nih.gov/tcga). *CKAP2L* mRNA expression was analyzed across multiple tumor types and corresponding normal tissues. Differential expression in TCGA cohorts was analyzed using DESeq2 (v1.36.0), with statistical significance defined as $|\log_2 FC| > 1$ and false discovery rate (FDR)-adjusted $p < 0.05$. Kaplan-Meier survival analyses were performed for overall survival (OS), progression-free survival (PFS), and post-progression survival (PPS). Statistical significance of survival differences was assessed by two-sided log-rank tests, and hazard ratios (HR) with 95% confidence intervals (CI) were calculated using Cox proportional hazards models. Unless otherwise stated, a nominal p-value < 0.05 was considered statistically significant.

Tumor Immune Estimation Resource (TIMER)

The TIMER database (https://cistrome.shinyapps.io/timer/) is a comprehensive resource for tumor immunology, enabling exploration and evaluation of immune infiltration. Correlations between *CKAP2L* expression and six types of tumor-infiltrating immune cells (TIICs) (B cells, $CD4^+$ T cells, $CD8^+$ T cells, neutrophils, macrophages, and dendritic cells) were obtained from the "GENE" module. The "Correlation" module was further used to analyze the relationship between *CKAP2L* expression and immune cell markers. Statistical analyses were conducted using purity-adjusted partial Spearman's correlation, with significance defined as FDR-adjusted $p < 0.05$. Gene expression levels were normalized and presented as $\log_2$ transcripts per million (TPM).

RNA Extraction and Quantitative Real-Time Polymerase Chain Reaction (qRT-PCR)

Total RNA was extracted from ovarian cancer cells (5×10^6) using TRIzol reagent (R0016, Biotop, Shanghai, China), following the manufacturer's instructions. 1 µg of total RNA was reverse transcribed using the SuperScript IV UniPrime One-Step RT-PCR System (12597500, Thermo Fisher Scientific, Waltham, MA, USA). The resulting cDNA served as a template for qRT-PCR. Amplification was conducted on an Applied Biosystems 7300 Real-Time PCR System (Applied Biosystems, Foster City, CA, USA) using the SuperScript™ III Platinum™ SYBR™ Green One-Step qRT-PCR Kit (11736051, Thermo Fisher Scientific, Waltham, MA, USA). Glyceraldehyde-3-phosphate dehydrogenase (GAPDH) was used as the internal control. Relative expression levels were calculated using the $2^{-\Delta\Delta CT}$ method [21]. Primers were synthesized by Sangon Biotech (Shanghai, China): *CKAP2L* (forward): 5′-GAGCCAAAACACCAAGCCTTA-3′, *CKAP2L* (reverse): 5′-GGAGTTTAATGCTGATGGACCTT-3′; *GAPDH* (forward): 5′-CATGAGAAGTATGACAACAGCCT-3′, *GAPDH* (reverse): 5′-AGTCCTTCCACGATACCAAAGT-3′. All experiments were performed in triplicate.

Cell Proliferation Assay

Cell proliferation was evaluated using the WST-1 Cell Proliferation Assay Kit (C0035, Beyotime, Shanghai, China). Ovarian cancer cells (2×10^3/well) were seeded into 96-well plates and incubated in culture medium for 24 hours per group. WST-1 solution (10 µL) was then added to each well and incubated for one hour according to the manufacturer's instructions. Absorbance was measured at 450 nm using a microplate reader v 6.0 (BioRad Laboratories, Hercules, CA, USA). Each experiment was performed with three independent replicates. Cell viability was determined as follows:

$$\text{Cell viability (\%)} = (OD_{experimental} - OD_{blank})/(OD_{control} - OD_{blank}) \times 100$$

Cell Migration Assay

Cell migration capacity was determined via the scratch assay. Ovarian cancer cells (5×10^5) were seeded into six-well plates and cultured until they reached 80–90% confluency. A 200 µL pipette tip was used to generate a scratch, followed by three washes with PBS. The cells were then incubated at 37 °C with 5% CO_2. Images of three distinct scratch sites were captured at 0 and 24 hours using a microscope (100×, Nikon Instruments Inc., Melville, NY, USA). Cell migration was quantified using ImageJ software (Version 1.53, National Institutes of Health, Bethesda, MD, USA). Each experiment was performed with three independent replicates.

Cell Apoptosis

Apoptosis was assessed by staining with Annexin V-fluorescein isothiocyanate (FITC) and propidium iodide (PI) (C1062, Biotop, Shanghai, China). Following the manufacturer's protocol, ovarian cancer cells (5×10^5) were harvested and stained with Annexin V-FITC and PI. Flow cytometric analysis was performed using an FACSCalibur cytometer (BD Biosciences, Franklin Lakes, NJ, USA). Each experiment was performed with three independent replicates.

Flow Cytometry

Ovarian cancer cells and PBMCs were isolated. PBMCs were washed twice with PBS and resuspended for immunophenotypic analysis. Fc receptor blocking solution (422301, BioLegend, San Diego, CA, USA) was added to PBMCs (5×10^6) and incubated for 10 minutes at 4

°C. Cells were stained for 30 minutes at 4 °C with allophycocyanin (APC)-conjugated anti-human CD11c antibody (980604, BioLegend, San Diego, CA, USA). Following permeabilization for 10 minutes with 1× Permeabilization Buffer (427705, BioLegend, San Diego, CA, USA), intracellular staining was performed for 30 minutes at 4 °C with fluorescein isothiocyanate (FITC)-conjugated anti-human CD206 antibody (321103, BioLegend, San Diego, CA, USA). Cells were washed with PBS and fixed with 1% paraformaldehyde (P0099, Biotop, Shanghai, China). Data were acquired using a flow cytometer and analyzed with FlowJo software (version 10.8.1, BD Biosciences, Ashland, OR, USA). Each experiment was performed with three independent replicates.

Western Blot Analysis

PBMCs (5×10^6) were lysed with RIPA buffer (89901, Thermo Fisher Scientific, Waltham, MA, USA), and the supernatant was collected after centrifugation at 12,000 rpm for 30 minutes at 4 °C. Protein concentration was determined using the Pierce™ Bicinchoninic Acid (BCA) Protein Assay Kits (23227, Thermo Fisher Scientific, Waltham, MA, USA). Protein samples were prepared with the Pierce™ SSDS-PAGE Sample Preparation Kits (10%, 89888, Thermo Fisher Scientific, Waltham, MA, USA), separated by electrophoresis, and transferred to polyvinylidene fluoride (PVDF) membranes (88518, Thermo Fisher Scientific, Waltham, MA, USA) using the Trans-Blot Transfer System. Membranes were blocked with 5% non-fat dry milk for 120 minutes at room temperature and incubated overnight at 4 °C with primary antibodies: anti-ADORA2A (5 µg/mL, 42 kDa, ab79714, Abcam, Cambridge, UK) and anti-GAPDH (5 µg/mL, 37 kDa, ab8245, Abcam, Cambridge, UK). After washing, membranes were incubated for 60 minutes at room temperature with goat anti-mouse IgG-HRP secondary antibody (1:2000, ab205719, Abcam, Cambridge, UK). Protein bands were visualized using enhanced Chemiluminescence (ECL) reagents (KGC4902, Keygene, Jiangsu, China) and imaged with a Bio-Rad gel documentation system (Hercules, CA, USA). GAPDH served as the loading control. Each experiment was performed with three independent replicates. Relative expression of the target protein was determined as follows:

Relative expression = (target protein band intensity)/(endogenous reference protein band intensity).

Cytokine Antibody Array

Ovarian cancer cells and PBMCs were co-cultured, and supernatants were collected. Three groups were defined: Con cancer cell + PBMC, siNC cancer cell + PBMC, and siCKAP2L cancer cell + PBMC. Cytokine expression was assessed using the Human Cytokine Array Q1 (QAH-CYT-1-1, RayBiotech Inc., Peachtree Corners, GA, USA), which detects multiple cytokines, including interleukin-1β (IL-1β), interleukin-10 (IL-10), and vascular endothelial growth factor (VEGF). Membranes were blocked with blocking buffer following the manufacturer's instructions and incubated overnight at 4 °C with culture supernatants. After washing, membranes were incubated with biotinylated antibody cocktails for two hours at room temperature, followed by incubation with Cy3-conjugated streptavidin for 1.5 hours at room temperature in the dark. Membranes were washed and scanned using a GenePix 4100A Scanner (Molecular Devices, San Jose, CA, USA). Slides were dried completely and rescanned within 24–48 hours at 10 µm resolution under optimized laser power and photon multiplier tube (PMT) settings. Signals were visualized using an enhanced chemiluminescence system (Amersham ImageQuant 800, Cytiva, Marlborough, MA, USA). Background signals were removed, and data were exported to Microsoft Excel for analysis. Each experiment was performed with three independent replicates.

Statistical Analysis

All quantitative experiments were repeated three times. Statistical analysis was conducted using GraphPad Prism 8.0 (GraphPad Software, Inc., San Diego, CA, USA). Data are expressed as mean ± standard deviation. Comparisons among multiple groups were performed using one-way ANOVA followed by Tukey's post hoc test. A p-value < 0.05 was considered statistically significant.

Results

Knockdown of CKAP2L Inhibits Ovarian Cancer Cell Proliferation and Migration and Promotes Apoptosis

qPCR analysis confirmed that CKAP2L knockdown significantly reduced *CKAP2L* expression in OVCAR3 and Caov-3 cells, with si-2 demonstrating the highest silencing efficiency. Therefore, si-2 was selected for subsequent experiments ($p < 0.001$, Fig. 1A,B). The WST-1 assay showed that CKAP2L knockdown markedly inhibited proliferation in OVCAR3 and Caov-3 ($p < 0.01$, Fig. 1C,D). Scratch assay results indicated that migration ability was significantly reduced in OVCAR3 and Caov-3 cells in the siCKAP2L group compared to the siNC group ($p < 0.01$, Fig. 1E–H). Flow cytometry further revealed a significant increase in apoptosis in OVCAR3 cells in the siCKAP2L group ($p < 0.001$, Fig. 2A,B), with similar results observed in Caov-3 cells ($p < 0.001$, Fig. 2C,D).

Knockdown of CKAP2L Suppresses M2 Polarization and Promotes M1 Polarization of Macrophages Induced by Ovarian Cancer Cells

TCGA database analysis showed that *CKAP2L* expression was significantly upregulated in ovarian cancer, cervical cancer, endometrial carcinoma, and other malignancies (Fig. 3A). In ovarian cancer, elevated *CKAP2L*

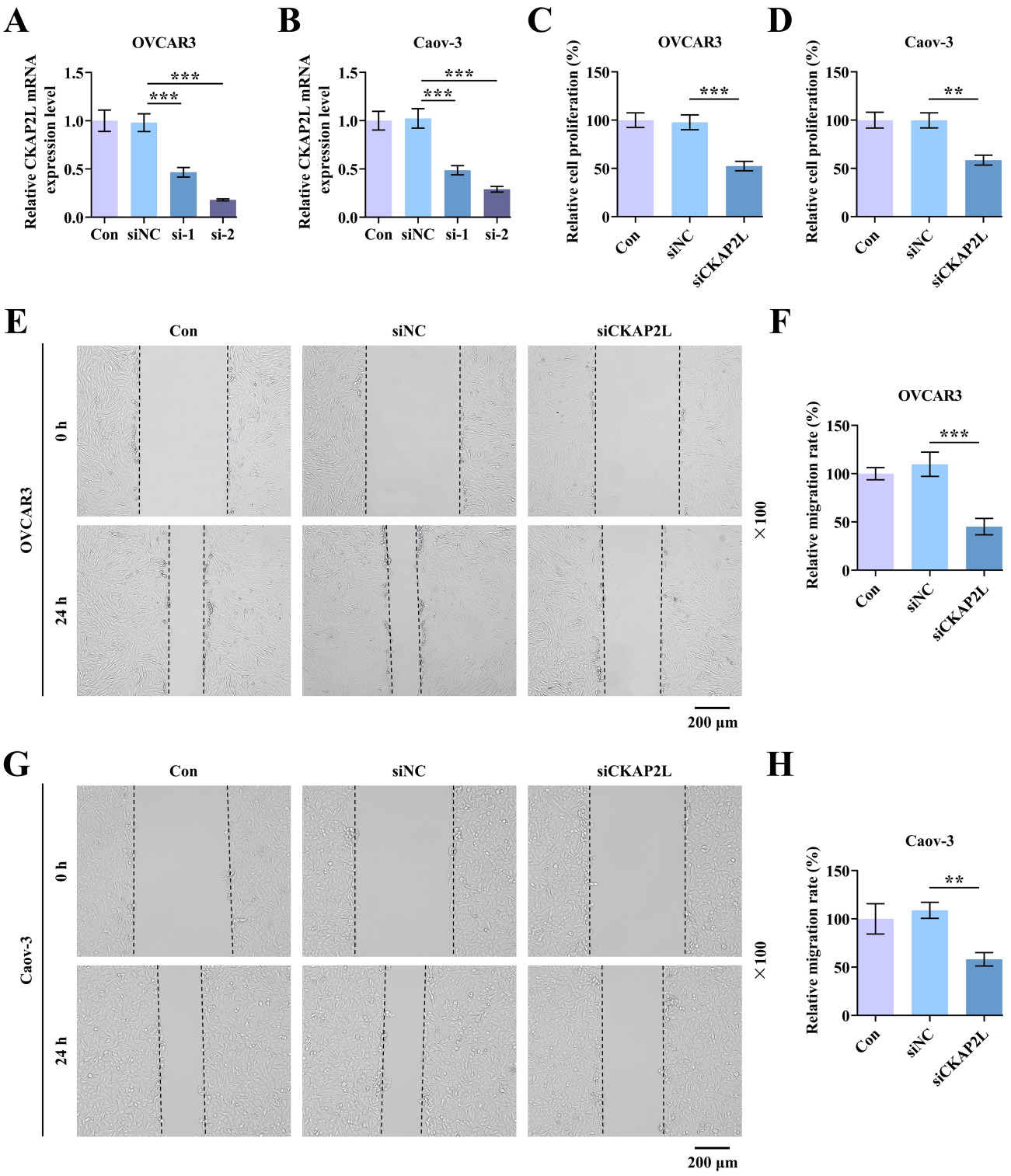

Fig. 1. Effects of Cytoskeleton-Associated Protein 2-Like (CKAP2L) knockdown on ovarian cancer cell proliferation and migration. (A,B) qRT-PCR analysis of *CKAP2L* in OVCAR3 and Caov-3 cells from the Con, siNC, and siCKAP2L groups. *GAPDH* served as the internal control. (C,D) WST-1 assays evaluating proliferation of OVCAR3 and Caov-3 cells in the Con, siNC, and siCKAP2L groups. (E–H) Scratch assays assessing migration of OVCAR3 and Caov-3 cells in the Con, siNC, and siCKAP2L groups. Magnification: 100×. Each experiment was performed in triplicate. $^{**}p < 0.01$, $^{***}p < 0.001$. n = 3 per group. Abbreviations: Con, control; siNC, negative control siRNA; siCKAP2L, small interfering RNA targeting CKAP2L; GAPDH, glyceraldehyde-3-phosphate dehydrogenase; qRT-PCR, quantitative real-time polymerase chain reaction.

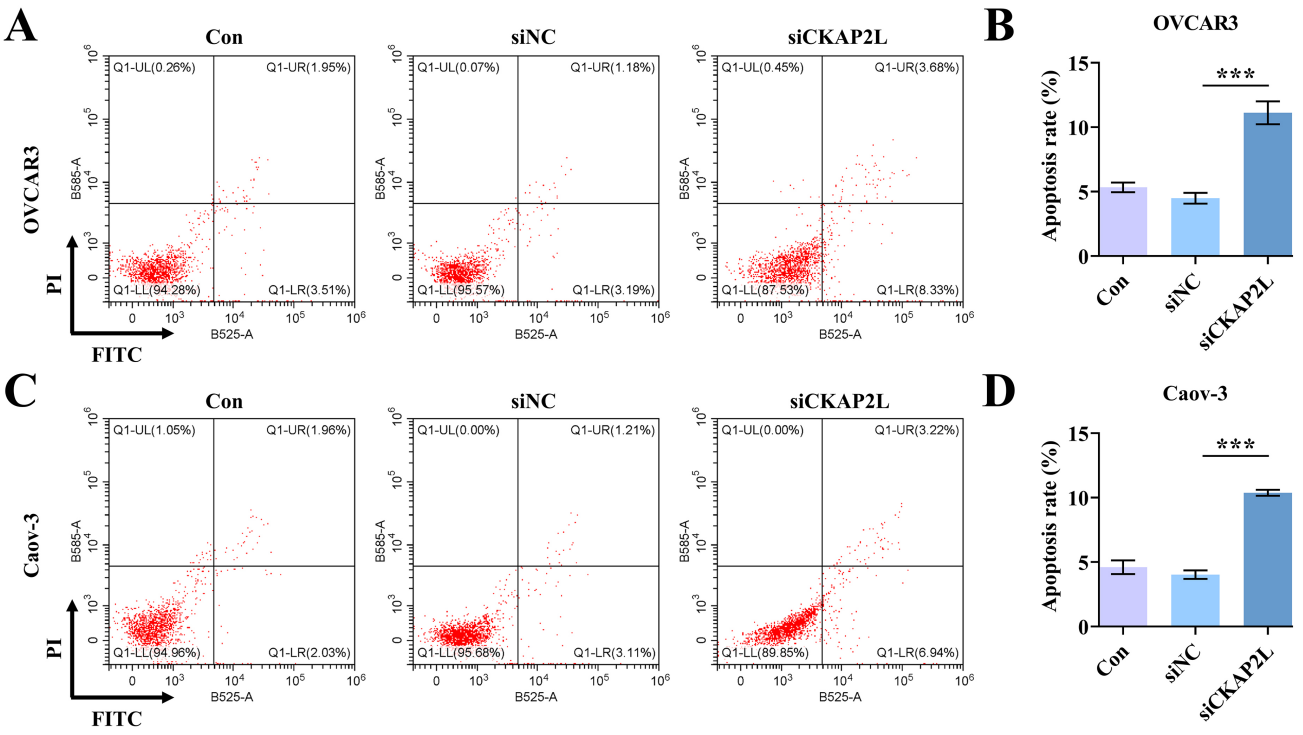

Fig. 2. Effects of CKAP2L knockdown on ovarian cancer cell apoptosis. (A,B) Flow cytometry analysis of apoptosis levels in OVCAR3 cells from the Con, siNC, and siCKAP2L groups. (C,D) Flow cytometry analysis of apoptosis levels in Caov-3 cells from the Con, siNC, and siCKAP2L groups. Each experiment was performed in triplicate. ***$p < 0.001$. n = 3 per group. Abbreviations: Con, control; siNC, negative control siRNA; siCKAP2L, small interfering RNA targeting CKAP2L.

expression was strongly associated with poor prognosis of ovarian cancer (Fig. 3B–D). TIMER database analysis showed that *CKAP2L* mRNA expression in ovarian carcinoma was significantly positively correlated with macrophage infiltration (Fig. 4, R = 0.174; $p = 0.000772$). Compared to the PBMC group, macrophages differentiated from PBMCs co-cultured with OVCAR3 cells showed increased expression in both $CD206^+$ (M2) and $CD11c^+$ (M1) markers ($p < 0.001$, Fig. 5A–C). CKAP2L knockdown reduced $CD206^+$ (M2) expression while further enhancing $CD11c^+$ (M1) levels ($p < 0.001$, Fig. 5A–C). Similar findings were observed in Caov-3 cells, where macrophages co-cultured with Caov-3 cells exhibited increased $CD206^+$ (M2) and $CD11c^+$ (M1) levels ($p < 0.001$, Fig. 5A,D,E). Compared to the siNC cancer cell + PBMC group, macrophages in the siCKAP2L cancer cell + PBMC group exhibited reduced $CD206^+$ (M2) levels and elevated $CD11c^+$ (M1) levels ($p < 0.001$, Fig. 5A,D,E).

Knockdown of CKAP2L Reduces ADORA2A Expression in Macrophages Induced by Ovarian Cancer Cells, Increases IL-1β, and Decreases IL-10 and VEGF

Western blot analysis revealed that ADORA2A protein levels in macrophages differentiated from PBMCs co-cultured with OVCAR3 and Caov-3 cells compared to the PBMC group ($p < 0.001$, Fig. 6A–C). However, ADORA2A expression was markedly lower in macrophages from the siCKAP2L cancer cell + PBMC group compared to the siNC cancer cell + PBMC group ($p < 0.001$, Fig. 6A–C). IL-1β, a characteristic cytokine of M1-type macrophages, along with IL-10 and VEGF, a secretory factor associated with M2-type macrophages, were assessed as polarization markers. CKAP2L knockdown significantly increased IL-1β levels while decreasing IL-10 and VEGF levels in the supernatants of OVCAR3 and Caov-3 cells co-cultured with PBMCs ($p < 0.01$, Fig. 6D–I).

Discussion

Through a series of functional assays, we observed that CKAP2L promotes ovarian cancer cell proliferation and migration while suppressing apoptosis. These findings suggest that CKAP2L plays a significant role in the pathogenesis of ovarian cancer. Macrophages are considered key immune effectors in tumor defense [22]. Previous study has shown that CKAP2L regulates the proliferation and apoptosis of esophageal squamous cell carcinoma by modulating the cell cycle [10]. Given that CKAP2L drives the cell cycle progression, it may indirectly contribute to the establishment of an immunosuppressive tumor microenvironment.

Increasing evidence indicates that the immune microenvironment plays a vital role in the development

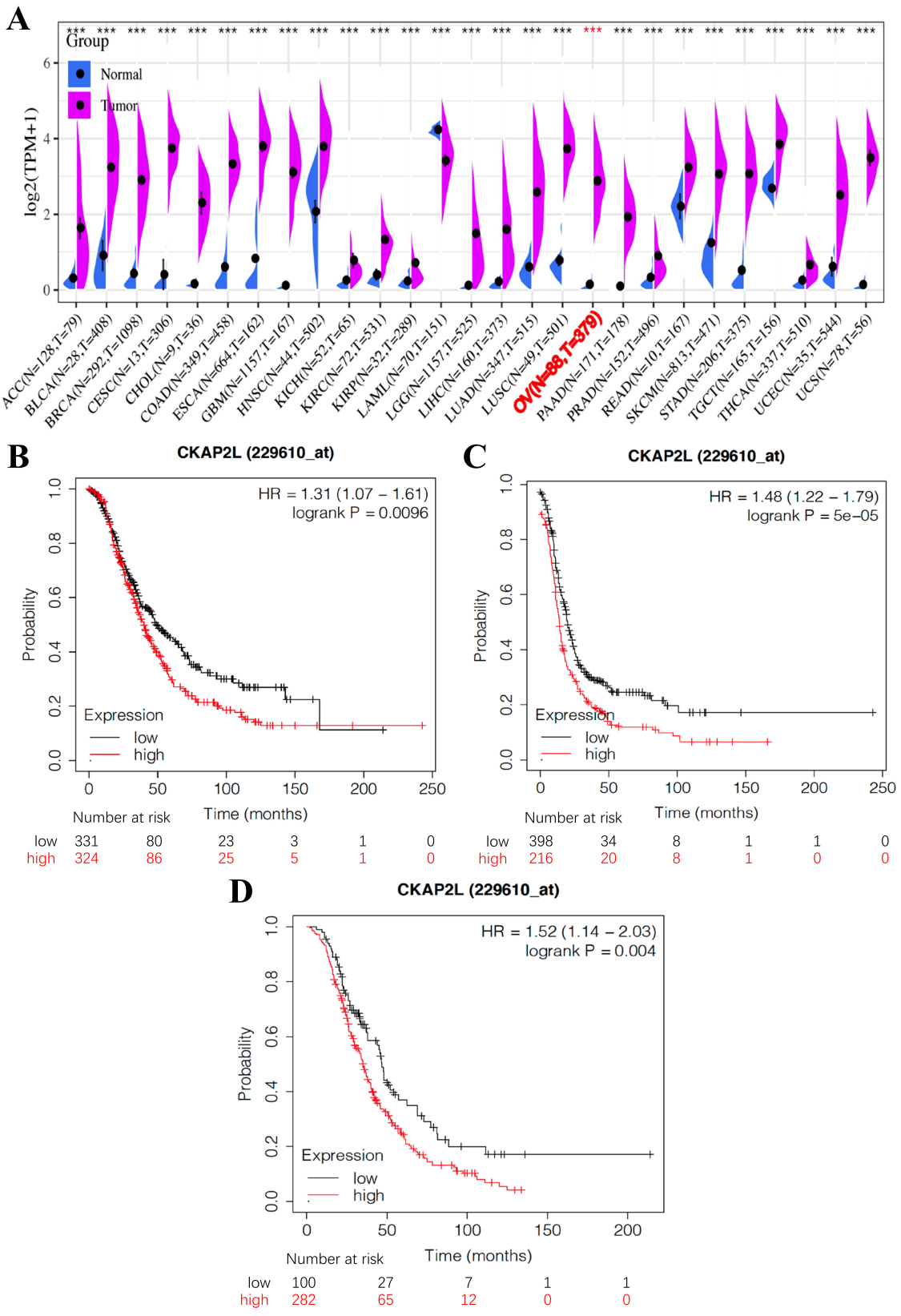

Fig. 3. Analysis of *CKAP2L* expression and prognosis in the TCGA database. (A) Expression of *CKAP2L* across multiple tumor types. The bold red font indicates that CKAP2L expression is significantly upregulated in ovarian cancer. (B–D) Association between *CKAP2L* mRNA expression and prognosis: overall survival (B), progression-free survival (C), and post-progression survival (D). ***$p < 0.001$. Abbreviations: TCGA, The Cancer Genome Atlas.

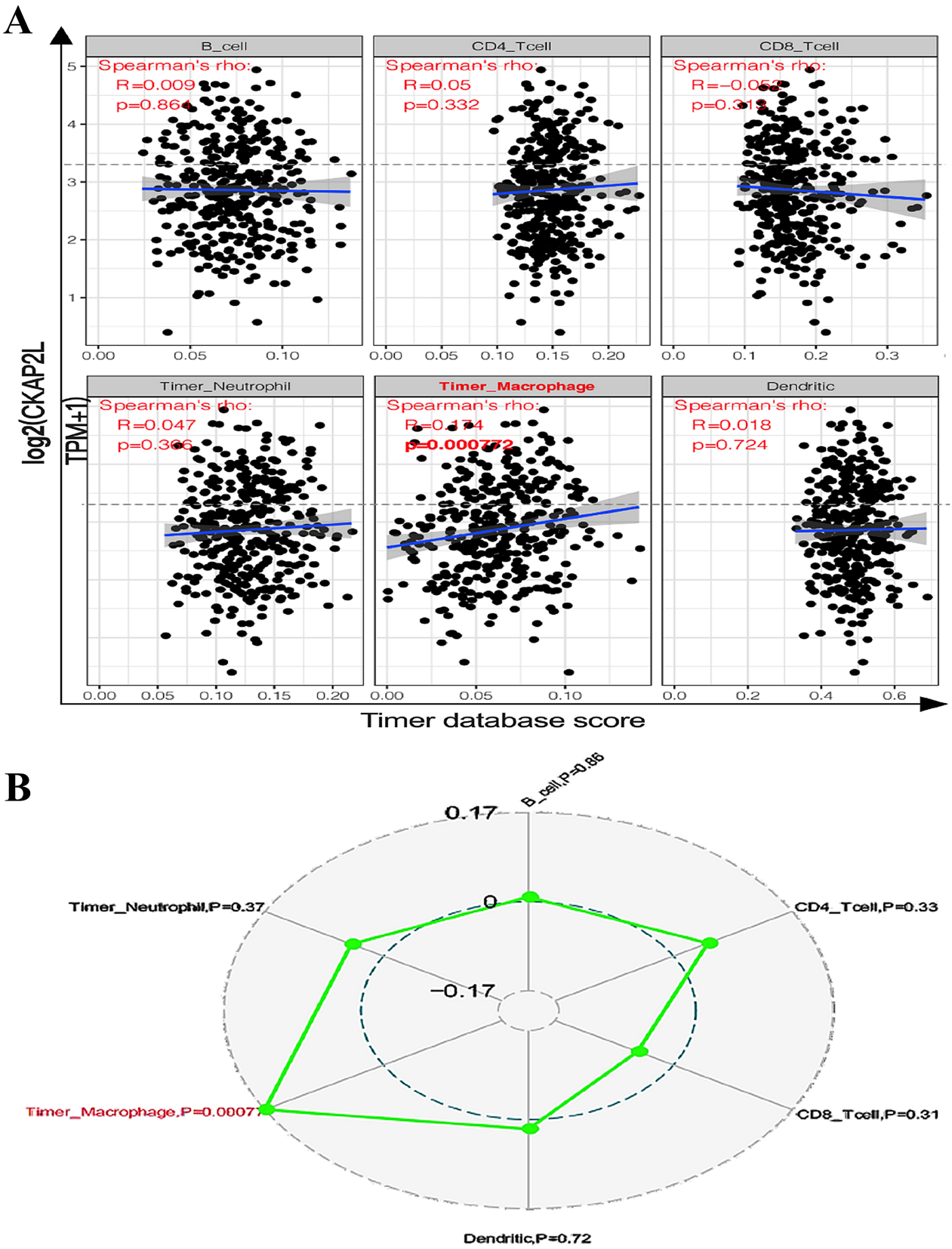

Fig. 4. Association between *CK2P2L* mRNA expression and macrophages in ovarian cancer based on the TIMER database. (A) Correlation coefficient and (B) *p*-value between immune cell scores and *CK2P2L* expression levels. The bold red font represents the *p*-value between CKAP2L expression levels and macrophage cells. Abbreviations: TIMER, Tumor Immune Estimation Resource.

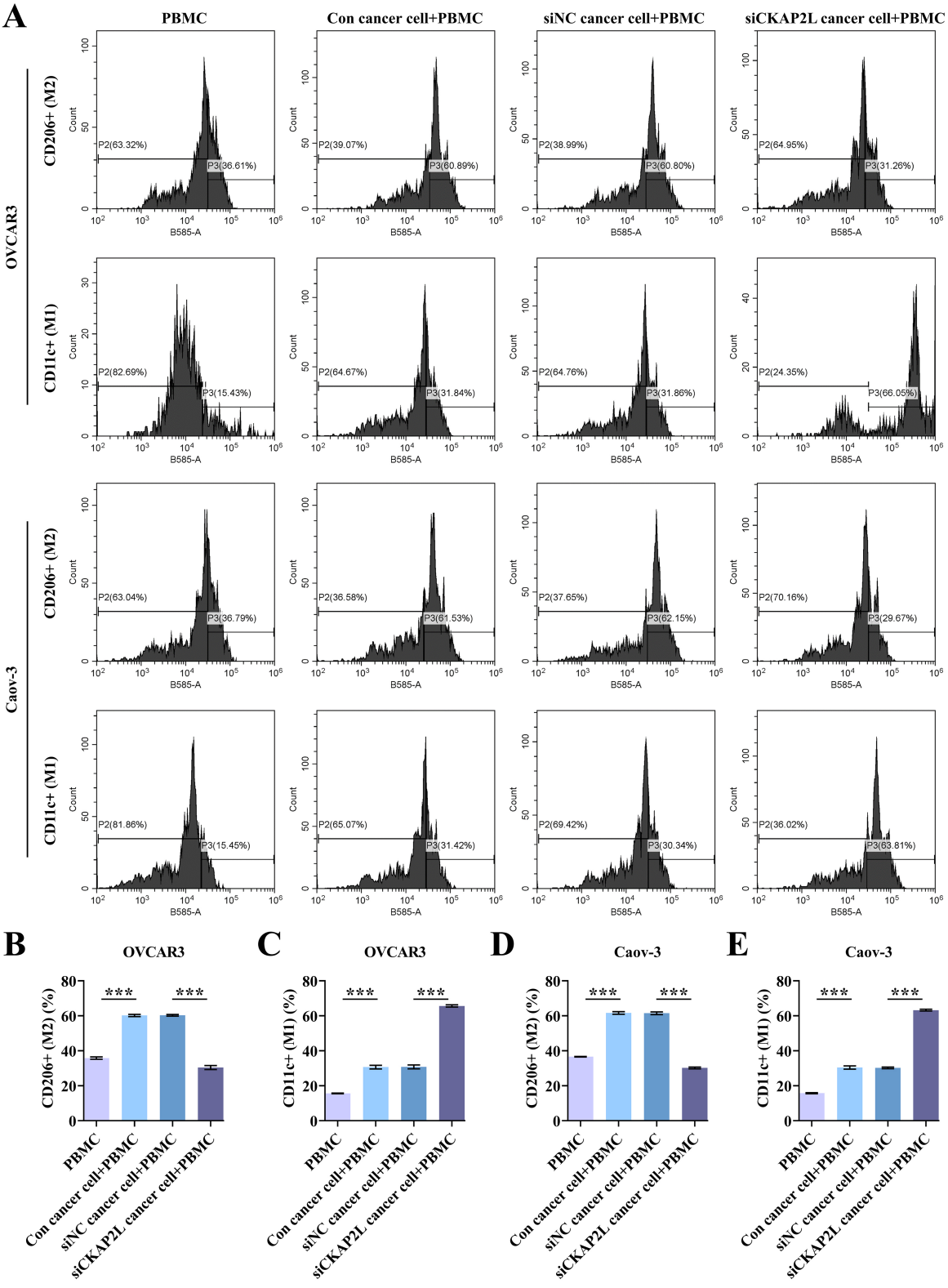

Fig. 5. Effects of CKAP2L knockdown on macrophage polarization induced by ovarian cancer cells. (A) Flow cytometry analysis of $CD206^+$ (M2) and $CD11c^+$ (M1) levels in macrophages differentiated from PBMCs in the PBMC, Con cancer cell + PBMC, siNC cancer cell + PBMC, and siCKAP2L cancer cell + PBMC groups. (B,C) Quantification of $CD206^+$ (M2) and $CD11c^+$ (M1) in macrophages differentiated from PBMCs co-cultured with OVCAR3 cells. (D,E) Quantification of $CD206^+$ (M2) and $CD11c^+$ (M1) in macrophages differentiated from PBMCs co-cultured with Caov-3 cells. Each experiment was performed in triplicate using flow cytometry. ***$p < 0.001$. n = 3 per group. Abbreviations: Con, control; siNC, negative control siRNA; siCKAP2L, small interfering RNA targeting CKAP2L; PBMCs, peripheral blood mononuclear cells.

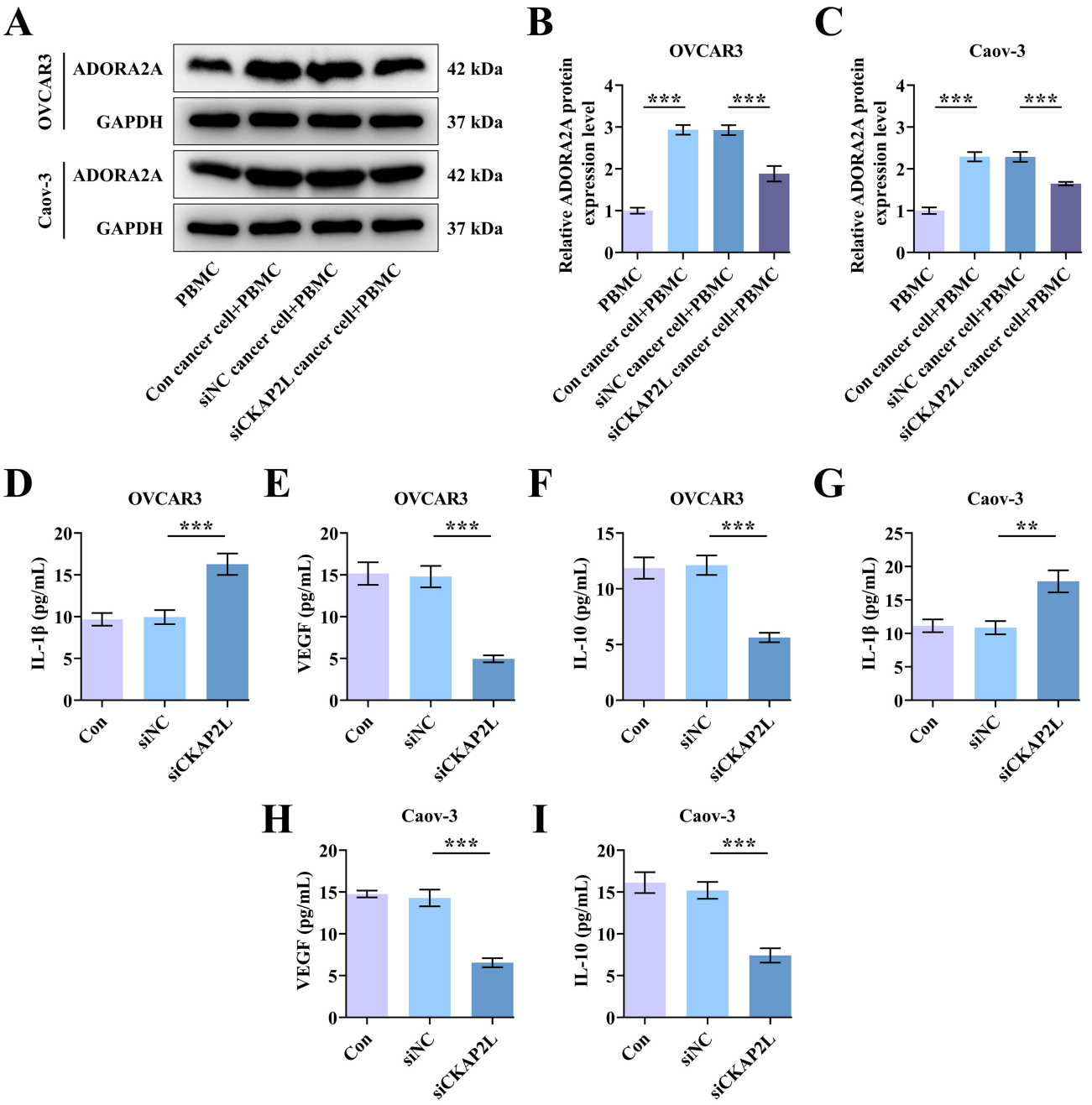

Fig. 6. Effects of CKAP2L knockdown on Adenosine A2A Receptor (ADORA2A) expression in PBMC-differentiated macrophages and cytokine regulation in ovarian cancer cells. (A–C) Western blot analysis of ADORA2A expression in macrophages differentiated from PBMCs in the PBMC, Con cancer cell + PBMC, siNC cancer cell + PBMC, and siCKAP2L cancer cell + PBMC groups. GAPDH served as the internal control. (D–F) IL-1β, IL-10, and VEGF levels in the supernatant of OVCAR3 cells co-cultured with PBMC from the Con, siNC, and siCKAP2L groups. (G–I) Cytokine antibody array analysis of IL-1β, IL-10, and VEGF levels in the supernatant of Caov-3 cells co-cultured with PBMC from the Con, siNC, and siCKAP2L groups. Each experiment was performed in triplicate. $^{**}p < 0.01$, $^{***}p < 0.001$. n = 3 per group. Abbreviations: Con, control; siNC, negative control siRNA; siCKAP2L, small interfering RNA targeting CKAP2L; IL-1β, interleukin-1β; IL-10, interleukin-10; VEGF, vascular endothelial growth factor.

and progression of ovarian cancer [23]. Analysis of the TIMER database revealed a significant association between CKAP2L mRNA expression and macrophage infiltration in ovarian cancer, while correlations with other immune cells were comparatively weaker. Accordingly, our functional experiments focused on macrophages, given both their established role in ovarian cancer progression and their strong bioinformatic association with CKAP2L.

Reports indicate that tumor-associated macrophages are the most abundant infiltrating immune cells in ovar-

ian tumors and ascites, and that their density and polarization status are strongly correlated with patient prognosis [8]. Tumor tissues recruit monocytes from peripheral circulation and drive their differentiation into tumor-associated macrophages, which predominantly exhibit M2 polarization features and functions. This polarization is a key mechanism underlying tumor immune evasion [24]. CD206 is commonly used as a marker of M2 macrophages, which primarily contribute to anti-inflammatory responses and tissue repair, including debris clearance, wound healing, and regulation of immune responses to promote healing [25,26]. Conversely, CD11c is a common marker of M1 macrophages, which are typically pro-inflammatory, secreting cytokines such as tumor necrosis factor-alpha (TNF-α) and interleukin-6 (IL-6) to promote antimicrobial and antiviral defense [27,28].

In the present study, macrophages differentiated from PBMCs co-cultured with ovarian cancer cells exhibited increased expression of both M1 and M2 markers, indicating that ovarian cancer cells may regulate the immune microenvironment by altering macrophage phenotypes to promote tumor progression. Notably, CKAP2L was shown to influence this polarization balance, promoting a shift from M1 toward M2 macrophages in ovarian cancer.

ADORA2A is a G protein-coupled receptor widely distributed throughout the body, primarily regulating diverse physiological functions through adenosine binding [29]. The oncogenic role of ADORA2A has been reported in multiple malignancies, though with tissue-specific differences. A previous study demonstrated that ADORA2A markedly inhibits neuroendocrine growth of prostate and lung cancer *in vivo* [30]. Zohair *et al.* [31] reported that ADORA2A is associated with invasive clinical outcomes in breast cancer, reflecting an immune-suppressive tumor microenvironment. Similarly, Zhang *et al.* [32] demonstrated that chuanliansu and paclitaxel synergistically suppress triple-negative breast cancer by regulating ADORA2A-EMT-related signaling pathway. Evidence suggests that ADORA2A strongly enhances macrophage activation, exerting a pivotal role in immune regulation and inflammatory responses [33]. Gao *et al.* [34] observed that jumonji domain-containing 3 (JMJD3) inhibits macrophage apoptosis by promoting ADORA2A expression in lipopolysaccharide (LPS)-induced acute lung injury. In psoriasis, ADORA2A activation suppresses M1 macrophage activation through the nuclear factor kappa B-keratin 16 (NF-κB-KRT16) pathway, reducing C-X-C motif chemokine ligand 10 and 11 (CXCL10/CXCL11) secretion and suppressing T helper 1 and 17 (Th1/Th17) differentiation [35].

In this study, we observed an increase in ADORA2A expression in macrophages differentiated from PBMCs induced by ovarian cancer cells, and this effect was suppressed by CKAP2L silencing. IL-1β is a major pro-inflammatory cytokine that promotes M1-type macrophage polarization, thereby enhancing pro-inflammatory responses [36]. Conversely, VEGF can influence macrophage activation status through VEGFR binding, frequently driving macrophage polarization toward the M2 phenotype [37]. Our findings demonstrate that CKAP2L suppresses IL-1β secretion in ovarian cancer cells while promoting IL-10 and VEGF secretion. These results suggest that ovarian cancer cells may regulate macrophage M2 polarization and the immune microenvironment by modulating IL-1β, IL-10, and VEGF secretion, as well as upregulating ADORA2A expression in macrophages.

This study has several limitations. First, all experiments were conducted *in vitro*, which, although providing valuable preliminary evidence, may not fully represent *in vivo* conditions. While our research clarifies the role of CKAP2L in ovarian cancer cells and the immune microenvironment, the precise molecular mechanisms and signaling pathways require further investigation. Future research will incorporate patient-derived organoids and xenografts to address this gap. Second, potential variability in PBMC responses due to donor heterogeneity remains a challenge. Future studies should use pooled PBMCs from multiple donors to minimize individual differences. Third, although we highlight the role of ADORA2A in macrophage phenotype regulation, its mechanistic interaction with CKAP2L remains unclear and constitutes a significant direction for future research. Finally, the current study focuses exclusively on the ovarian cancer cell lines OVCAR3 and Caov-3, and the findings may not be generalizable across all ovarian cancer subtypes or patient populations.

Conclusions

In conclusion, this study highlights the critical role of CKAP2L in ovarian cancer. We demonstrated that CKAP2L accelerates *in vitro* ovarian cancer progression by enhancing cell proliferation and migration while suppressing apoptosis. CKAP2L also modulates cytokine secretion by ovarian cancer cells, reducing IL-1β production and increasing IL-10, VEGF release. Furthermore, CKAP2L promotes macrophage polarization toward the M2 phenotype induced by ovarian cancer cells and elevates ADORA2A expression. Collectively, these findings provide valuable insights into how ovarian cancer regulates the immune microenvironment to support tumor growth and metastasis.

Availability of Data and Materials

The datasets used and/or analyzed during the current study are available from the corresponding author upon reasonable request.

Author Contributions

Substantial contributions to conception and design: HKS, ZYR. Data acquisition, data analysis and interpretation: JNL, ZLY. Drafting the article: HKS. Critically revising it for important intellectual content: All authors. Final approval of the version to be published: All authors. Agreement to be accountable for all aspects of the work in ensuring that questions related to the accuracy or integrity of the work are appropriately investigated and resolved: All authors.

Ethics Approval and Consent to Participate

Not applicable.

Acknowledgment

Not applicable.

Funding

This research received no external funding.

Conflict of Interest

The authors declare no conflict of interest.

References

[1] Nasser S, El Bairi K, Trapani D, Efared B. Origins and Pathology of Epithelial Ovarian Cancer: A Brief Overview. Ovarian Cancer Biomarkers: Mapping to Improve Outcomes (pp. 1–17). Springer: Singapore. 2021. https://doi.org/10.1007/978-981-16-1873-4_1.

[2] Feng J, Xu L, Chen Y, Lin R, Li H, He H. Trends in incidence and mortality for ovarian cancer in China from 1990 to 2019 and its forecasted levels in 30 years. Journal of Ovarian Research. 2023; 16: 139. https://doi.org/10.1186/s13048-023-01233-y.

[3] Ali AT, Al-Ani O, Al-Ani F. Epidemiology and risk factors for ovarian cancer. Przeglad Menopauzalny = Menopause Review. 2023; 22: 93–104. https://doi.org/10.5114/pm.2023.128661.

[4] Sartorius CM, Heinzelmann-Schwarz V. Diagnosis of Epithelial Ovarian, Fallopian Tubal and Peritoneal Surface Cancers. The EBCOG Postgraduate Textbook of Obstetrics & Gynaecology: Gynaecology. 2021; 2: 348–356. https://doi.org/10.1017/9781108582322.042.

[5] Della Corte L, Foreste V, Di Filippo C, Giampaolino P, Bifulco G. Poly (ADP-ribose) polymerase (PARP) as target for the treatment of epithelial ovarian cancer: what to know. Expert Opinion on Investigational Drugs. 2021; 30: 543–554. https://doi.org/10.1080/13543784.2021.1901882.

[6] Vanacker H, Harter P, Labidi-Galy SI, Banerjee S, Oaknin A, Lorusso D, *et al*. PARP-inhibitors in epithelial ovarian cancer: Actual positioning and future expectations. Cancer Treatment Reviews. 2021; 99: 102255. https://doi.org/10.1016/j.ctrv.2021.102255.

[7] Bagchi S, Yuan R, Engleman EG. Immune Checkpoint Inhibitors for the Treatment of Cancer: Clinical Impact and Mechanisms of Response and Resistance. Annual Review of Pathology. 2021; 16: 223–249. https://doi.org/10.1146/annurev-pathol-042020-042741.

[8] El-Arabey AA, Alkhalil SS, Al-Shouli ST, Awadalla ME, Alhamdi HW, Almanaa TN, *et al*. Revisiting macrophages in ovarian cancer microenvironment: development, function and interaction. Medical Oncology (Northwood, London, England). 2023; 40: 142. https://doi.org/10.1007/s12032-023-01987-x.

[9] Monteverde T, Sahoo S, La Montagna M, Magee P, Shi L, Lee D, *et al*. CKAP2L Promotes Non-Small Cell Lung Cancer Progression through Regulation of Transcription Elongation. Cancer Research. 2021; 81: 1719–1731. https://doi.org/10.1158/0008-5472.CAN-20-1968.

[10] Chen W, Wang Y, Wang L, Zhao H, Li X. CKAP2L Promotes Esophageal Squamous Cell Carcinoma Progression and Drug-Resistance by Modulating Cell Cycle. Journal of Oncology. 2022; 2022: 2378253. https://doi.org/10.1155/2022/2378253.

[11] Paim LMG, Lopez-Jauregui AA, McAlear TS, Bechstedt S. The spindle protein CKAP2 regulates microtubule dynamics and ensures faithful chromosome segregation. Proceedings of the National Academy of Sciences of the United States of America. 2024; 121: e2318782121. https://doi.org/10.1073/pnas.2318782121.

[12] Chi F, Chen L, Jin X, He G, Liu Z, Han S. CKAP2L, transcriptionally inhibited by FOXP3, promotes breast carcinogenesis through the AKT/mTOR pathway. Experimental Cell Research. 2022; 412: 113035. https://doi.org/10.1016/j.yexcr.2022.113035.

[13] Geier C, Perl A. Therapeutic mTOR blockade in systemic autoimmunity: Implications for antiviral immunity and extension of lifespan. Autoimmunity Reviews. 2021; 20: 102984. https://doi.org/10.1016/j.autrev.2021.102984.

[14] Zhu L, Zheng Y, Hu R, Hu C. *CKAP2L*, as an Independent Risk Factor, Closely Related to the Prognosis of Glioma. BioMed Research International. 2021; 2021: 5486131. https://doi.org/10.1155/2021/5486131.

[15] Shi Y, Xiong X, Sun Y, Geng Z, Chen X, Cui X, *et al*. IGF2BP2 promotes ovarian cancer growth and metastasis by upregulating CKAP2L protein expression in an m^6 A-dependent manner. FASEB Journal: Official Publication of the Federation of American Societies for Experimental Biology. 2023; 37: e23183. https://doi.org/10.1096/fj.202202145RRR.

[16] Wang X, Qian X, Zhao D, Xu R, Liu Z. Role of *KIF20A* Depletion in Inhibiting Ovarian Cancer Progression: Insights From *PTEN* and M2 Macrophage Polarization. Discovery Medicine. 2024; 36: 2433–2444. https://doi.org/10.24976/Discov.Med.202436191.224.

[17] Lin H, Lan KC, Ou YC, Wu CH, Kang HY, Chuang IC, *et al*. Highly Expressed Progesterone Receptor B Isoform Increases Platinum Sensitivity and Survival of Ovarian High-Grade Serous Carcinoma. Cancers. 2021; 13: 5578. https://doi.org/10.3390/cancers13215578.

[18] Mitra AK, Davis DA, Tomar S, Roy L, Gurler H, Xie J, *et al*. In vivo tumor growth of high-grade serous ovarian cancer cell lines. Gynecologic Oncology. 2015; 138: 372–377. https://doi.org/10.1016/j.ygyno.2015.05.040.

[19] Sánchez-Reyes K, Bravo-Cuellar A, Hernández-Flores G, Lerma-Díaz JM, Jave-Suárez LF, Gómez-Lomelí P, *et al*. Cervical cancer cell supernatants induce a phenotypic switch from U937-derived macrophage-activated M1 state into M2-like suppressor phenotype with change in Toll-like receptor profile. BioMed Research International. 2014; 2014: 683068. https://doi.org/10.1155/2014/683068.

[20] Li L, Yu S, Zang C. Low Necroptosis Process Predicts Poor Treatment Outcome of Human Papillomavirus Positive Cervical Cancers by Decreasing Tumor-Associated Macrophages M1 Polarization. Gynecologic and Obstetric Investigation. 2018; 83: 259–267. https://doi.org/10.1159/000487434.

[21] Maren NA, Duduit JR, Huang D, Zhao F, Ranney TG, Liu W.

Stepwise Optimization of Real-Time RT-PCR Analysis. Methods in Molecular Biology (Clifton, N.J.). 2023; 2653: 317–332. https://doi.org/10.1007/978-1-0716-3131-7_20.

[22] Yan S, Wan G. Tumor-associated macrophages in immunotherapy. The FEBS Journal. 2021; 288: 6174–6186. https://doi.org/10.1111/febs.15726.

[23] Almeida-Nunes DL, Mendes-Frias A, Silvestre R, Dinis-Oliveira RJ, Ricardo S. Immune Tumor Microenvironment in Ovarian Cancer Ascites. International Journal of Molecular Sciences. 2022; 23: 10692. https://doi.org/10.3390/ijms231810692.

[24] Wang H, Yung MMH, Ngan HYS, Chan KKL, Chan DW. The Impact of the Tumor Microenvironment on Macrophage Polarization in Cancer Metastatic Progression. International Journal of Molecular Sciences. 2021; 22: 6560. https://doi.org/10.3390/ijms22126560.

[25] Song J, Xiao T, Li M, Jia Q. Tumor-associated macrophages: Potential therapeutic targets and diagnostic markers in cancer. Pathology, Research and Practice. 2023; 249: 154739. https://doi.org/10.1016/j.prp.2023.154739.

[26] Mao J, Chen L, Cai Z, Qian S, Liu Z, Zhao B, *et al*. Advanced biomaterials for regulating polarization of macrophages in wound healing. Advanced Functional Materials. 2022; 32: 2111003. https://doi.org/10.1002/adfm.202111003.

[27] Sari S, Özdemir Ç, Çilekar M. The relationship of tumour-associated macrophages (CD68, CD163, CD11c) and cancer stem cell (CD44) markers with prognostic parameters in breast carcinomas. Polish Journal of Pathology: Official Journal of the Polish Society of Pathologists. 2022; 73: 299–309. https://doi.org/10.5114/pjp.2022.125424.

[28] Kadomoto S, Izumi K, Mizokami A. Macrophage Polarity and Disease Control. International Journal of Molecular Sciences. 2021; 23: 144. https://doi.org/10.3390/ijms23010144.

[29] Garcia CP, Licht-Murava A, Orr AG. Effects of adenosine A_{2A} receptors on cognitive function in health and disease. International Review of Neurobiology. 2023; 170: 121–154. https://doi.org/10.1016/bs.irn.2023.04.006.

[30] Jing N, Zhang K, Chen X, Liu K, Wang J, Xiao L, *et al*. ADORA2A-driven proline synthesis triggers epigenetic reprogramming in neuroendocrine prostate and lung cancers. The Journal of Clinical Investigation. 2023; 133: e168670. https://doi.org/10.1172/JCI168670.

[31] Zohair B, Chraa D, Rezouki I, Benthami H, Razzouki I, Elkarroumi M, *et al*. The immune checkpoint adenosine 2A receptor is associated with aggressive clinical outcomes and reflects an immunosuppressive tumor microenvironment in human breast cancer. Frontiers in Immunology. 2023; 14: 1201632. https://doi.org/10.3389/fimmu.2023.1201632.

[32] Zhang J, Xu HX, Wu YL, Cho WCS, Xian YF, Lin ZX. Synergistic Anti-Tumor Effect of Toosendanin and Paclitaxel on Triple-Negative Breast Cancer via Regulating ADORA2A-EMT Related Signaling. Advanced Biology. 2023; 7: e2300062. https://doi.org/10.1002/adbi.202300062.

[33] Cekic C, Day YJ, Sag D, Linden J. Myeloid expression of adenosine A2A receptor suppresses T and NK cell responses in the solid tumor microenvironment. Cancer Research. 2014; 74: 7250–7259. https://doi.org/10.1158/0008-5472.CAN-13-3583.

[34] Gao Y, Wang N, Jia D. H3K27 tri-demethylase JMJD3 inhibits macrophage apoptosis by promoting ADORA2A in lipopolysaccharide-induced acute lung injury. Cell Death Discovery. 2022; 8: 475. https://doi.org/10.1038/s41420-022-01268-y.

[35] Lu Y, Zhu W, Zhang GX, Chen JC, Wang QL, Mao MY, *et al*. Adenosine A2A receptor activation regulates the M1 macrophages activation to initiate innate and adaptive immunity in psoriasis. Clinical Immunology (Orlando, Fla.). 2024; 266: 110309. https://doi.org/10.1016/j.clim.2024.110309.

[36] Zhu L, Zhao Q, Yang T, Ding W, Zhao Y. Cellular metabolism and macrophage functional polarization. International Reviews of Immunology. 2015; 34: 82–100. https://doi.org/10.3109/08830185.2014.969421.

[37] Zhang Y, Brekken RA. Direct and indirect regulation of the tumor immune microenvironment by VEGF. Journal of Leukocyte Biology. 2022; 111: 1269–1286. https://doi.org/10.1002/JLB.5RU0222-082R.